[3] Forsberg, K. J., "Assessment of Current Methods for Dynamic Analysis of Complex Structures," TM X-52876, Vol. II, July 1970, NASA, pp. 4–27.
[4] Lazan, B. J., *Damping of Materials and Members in Structural Mechanics*, Pergamon Press, New York, 1968.
[5] Snowdon, J. C., *Vibration and Shock in Damped Mechanical Systems*, Wiley, New York, 1968.
[6] Steidel, R. F., Jr., *An Introduction to Mechanical Vibrations*, Wiley, New York, 1971.
[7] Kana, D. D. and Huzar, S., "Synthesis of Shuttle Vehicle Damping Using Substructure Test Results," Interim Report, Contract NAS8-27569, June 1972, Southwest Research Institute, San Antonio, Texas.

DECEMBER 1973 J. SPACECRAFT VOL. 10, NO. 12

Similarity Analysis for the Surface Ablation of Silica-Reinforced Composites

CHIA-LUNG HSIEH* AND J. D. SEADER†
University of Utah, Salt Lake City, Utah

The ablation mechanism of a silica-reinforced composite is approximated as a problem involving a two-phase laminar boundary-layer melt flow with heterogeneous chemical reaction. A model of mixture flow is used to simplify the governing equations, which are converted into a set of ordinary differential equations via similarity transforms. The technique of quasilinearization is utilized to attack this coupled boundary-value problem. It is found that this numerical procedure can converge rapidly to the true solution, if the dimensionless variables and the boundary conditions are properly defined. This is achieved by analyzing the physical nature of the ablation mechanism and the stability and convergence characteristics of the governing equations. The strategy of matching the interface conditions of the molten layer and the gas-boundary layer is also developed, after the solution of the gas boundary-layer flow is analyzed.

Nomenclature

B = dimensionless void fraction $(1-\phi)/(1-\phi_0)$
Cp = specific heat, cal/gm°K
E = activation energy, cal/mole
f = dimensionless stream function
h = specific enthalpy, cal/gm
H_{eff}, H_f, H_p, H_R = heats of ablation, fusion, pyrolysis, reaction, cal/gm
j = volumetric average velocity of the two-phase flow, cm/sec
K = thermal conductivity, cal/sec cm°K
K_e = effective thermal conductivity of the molten layer, cal/sec cm°K
K_R = reaction rate constant, gm/cm² sec
$\dot{m}_a$ = ablation rate, or rate of formation of char, gm/sec cm²
$\dot{m}_l$ = mass transfer rate at the molten layer interface, gm/sec cm²
$\dot{m}_p$ = rate of pyrolysis, gm/sec cm²
$\dot{m}_R$ = rate of carbon-silica reaction, gm/sec cm²
M = ratio of molecular weight of gas-phase to air
n = exponential coefficient of viscosity
p = pressure, atm
Pr = Prandtl number
q = heat transfer rate, cal/cm² sec
q_c = conductive heat transfer rate, cal/cm² sec
q_s = heat transfer rate to the non-ablative surface, cal/cm² sec.
r = body dimension measured normal to the axis of revolution, cm
R = gas constant, 1.987 cal/g-mole °K
R_b = radius of the blunt body, cm
T = temperature, °K
T_r = reference temperature, °K
ΔT = $T_i - T_o$, °K
u = velocity component in the x-direction, cm/sec
u_e = velocity at the edge of the gas boundary-layer, cm/sec/
u_{gj} = drift velocity of the gas-phase in the x-direction, cm/sec
v = velocity component in the y-direction, cm/sec
v_{gj} = drift velocity of the gas-phase in the y-direction, cm/sec
w = mass fraction of the pyrolysis gases
x = coordinate parallel to the body surface, cm
y = coordinate normal to the body surface, cm
β = volume fraction of the liquid phase, $(1-\phi)$
ε = geometric constant
η = dimensionless y-coordinate
θ = dimensionless temperature
μ = viscosity, gm/cm sec
μ_m = apparent viscosity of gas-liquid mixture, gm/cm sec
μ^* = dimensionless apparent viscosity
ρ = density, gm/cm³
$\tilde{s}$ = dimensionless x-coordinate
τ = shear stress, dyne/cm²
ϕ = void fraction of the gas-phase
ψ = stream function, also coefficient of blocking effect

Subscripts

G = gas-phase of the molten layer
i = gas-liquid interface

Received April 19, 1973; revision received August 8, 1973. This study was supported by the AFOSR under Contract F44620-68-C-0022.
Index category: Material Ablation.
* Now Project Engineer, the Amalgamated Sugar Company, Ogden, Utah.
† Professor of Chemical Engineering. Member AIAA.

L = liquid-phase of the molten layer
o = liquid-char interface
r = reference temperature
s = stagnation point of the blunt body
w = char
x = component in the x-direction
y = component in the y-direction

Introduction

SINCE the early development of ablation theory, the technique of similarity transforms[1-3] has been considered the most accurate method of solution. In this study, a systematic procedure was developed for obtaining a more complete solution of the ablation mechanism of silica-reinforced composites than previously reported.

The ablation mechanism of phenolic-silica composites is analyzed here. Figure 1 is a schematic diagram of the assumed ablation mechanism. When such an ablative material is subjected to high heat flux, the phenolic resin within the composite will at first pyrolyze. As the pyrolysis proceeds, the decomposition zone will recess and penetrate into the interior of the material. The products of the pyrolysis are a mixture of gases and a residual char layer of mainly carbon and silica. If the heat flux is very large, the silica fiber within the char will eventually melt and form a liquid film covering the surface of the char. The pyrolysis gases will then percolate through the char and then bubble through the molten layer. In this process, complex post-pyrolytic chemical reactions may also take place. Near the surface of the molten layer, heterogeneous carbon-silica reactions may occur. In addition, molten silica may be subject to vaporization.

Governing Equations

It was found that the above mechanism can be best characterized by a two-phase laminar boundary-layer flow with heterogeneous chemical reactions taking place at both boundaries of the molten layer. The governing equations which represent this mechanism are[4]

a) Continuity Equation of Liquid

$$\frac{\partial[u_L(1-\phi)r^\epsilon]}{\partial x}+\frac{\partial[v_L(1-\phi)r^\epsilon]}{\partial y}=0 \tag{1}$$

b) Momentum Equations

$$(1-\phi)\rho_L\left(u_L\frac{\partial u_L}{\partial x}+v_L\frac{\partial u_L}{\partial y}\right)=-\frac{\partial p}{\partial x}+\frac{\partial}{\partial y}\left(\mu_m\frac{\partial j_x}{\partial y}\right) \tag{2}$$

$$\partial p/\partial y=0 \tag{3}$$

c) Energy Equation

$$(1-\phi)\rho_L C p_L\left(u_L\frac{\partial T}{\partial x}+v_L\frac{\partial T}{\partial y}\right)=\frac{\partial}{\partial y}\left(K_e\frac{\partial T}{\partial y}\right) \tag{4}$$

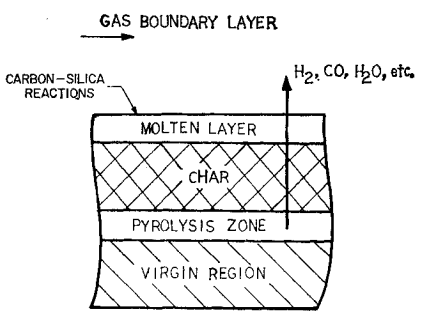

Fig. 1 Ablation mechanism of reinforced composites.

d) Void Propagation Equation[5]

$$j_x\left(\frac{\partial\phi}{\partial x}\right)+(j_y+v_{gj})\frac{\partial\phi}{\partial y}=-\phi(1-\phi)\left(\frac{u_G}{\rho_G}\frac{\partial\rho_G}{\partial x}+\frac{v_G}{\rho_G}\frac{\partial\rho_G}{\partial y}\right) \tag{5}$$

where

$$j_x=(1-\phi)u_L+\phi u_G \tag{6}$$

$$j_y=(1-\phi)v_L+\phi v_G \tag{7}$$

$$u_{gj}=u_G-j_x \tag{8}$$

$$v_{gj}=v_G-j_y \tag{9}$$

The coordinate system for the above equations is shown in Fig. 2. The x-axis is the interface between the molten layer and the gas boundary layer. The y-axis is perpendicular to the x-axis.

In the above equations, μ_m and K_e represent the apparent viscosity and the effective thermal conductivity of the molten layer, respectively. These two quantities can be estimated by the following relations[4]

$$K_e=K_L(1-(3/2)\phi) \tag{10}$$

$$\mu_m=\mu_r(1-K\phi)(T/T_r)^{-n} \tag{11}$$

where $-1.0\leq K\leq 2.5$. The boundary conditions for the above equations are

at $y=0$: $v_L=v_i$, $-\mu_m(\partial j_x/\partial y)=\tau_i$ and $T=T_i$

and at $y\to-\infty$: $u_L=0$, $T=T_o$, $\phi=\phi_o$

It should be noted that the previous investigators[2,3] assigned quantitative values to the boundary conditions at $y=0$. In fact, in any ablation process, these values are all unknown and can only be obtained through a matching of the interface conditions between the molten layer and the gas boundary layer. In this analysis the latter approach was adopted.

Model of Mixture Flow

Two gas-bubble drag equations were required to complete the above set of governing equations.[6] However, instead of obtaining the analytical solution to these two equations, mathematical models can be postulated, and the drift velocities of the gas bubbles can be regarded as parameters. In this study, the model of mixture flow[7] was utilized. Solutions for other mathematical models could be obtained by following the same procedure of this study.

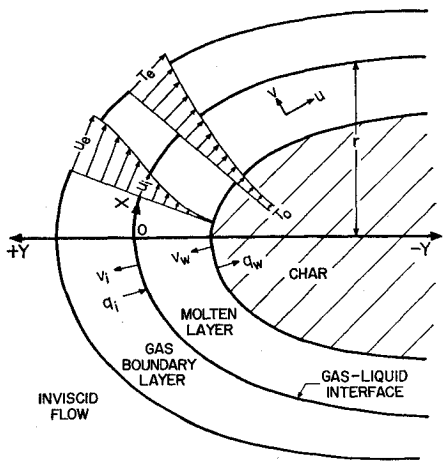

Fig. 2 Coordinate system for axisymmetric bodies.

According to the model of mixture flow, it is assumed that, within the molten layer, the distribution of suspended gas bubbles may not be homogeneous. But, the drift velocities of any gas bubble, relative to the surrounding liquid, are zero. Consequently, the governing equations were simplified to

a) Continuity of Liquid Phase

$$\frac{\partial(\beta u r^{\varepsilon})}{\partial x} + \frac{\partial(\beta v r^{\varepsilon})}{\partial y} = 0 \tag{12}$$

b) Momentum Equation

$$\beta\rho_L\left(u\frac{\partial u}{\partial x} + v\frac{\partial u}{\partial y}\right) = -\frac{\partial p}{\partial x} + \frac{\partial}{\partial y}\left(\mu_m\frac{\partial u}{\partial y}\right) \tag{13}$$

c) Energy Equation

$$\beta\rho_L\, Cp_L\left(u\frac{\partial T}{\partial x} + v\frac{\partial T}{\partial y}\right) = \frac{\partial}{\partial y}\left(K_e\frac{\partial T}{\partial y}\right) \tag{14}$$

d) Void-propagation Equation

$$\rho_G\left(u\frac{\partial\beta}{\partial x} + v\frac{\partial\beta}{\partial y}\right) = \beta(1-\beta)\left(u\frac{\partial\rho_G}{\partial y} + v\frac{\partial\rho_G}{\partial y}\right) \tag{15}$$

where $\beta = 1 - \phi$

Similarity Transforms and Linearization

By the technique of separation of variables[8], the above governing equations were converted into a set of ordinary differential equations by using the following similarity transforms[4]

$$\tilde{s} = \rho_L\mu_r\beta_o\int_0^x u_e r^{2\varepsilon}dx \tag{16}$$

$$\eta = \frac{\rho_L\beta_o u_e r^{\varepsilon}}{(2\tilde{s})^{1/2}}\int_0^y B dy \tag{17}$$

$$\frac{\partial\psi}{\partial y} = \rho_L(1-\phi)ur^{\varepsilon} \tag{18}$$

$$-\frac{\partial\psi}{\partial x} = \rho_L(1-\phi)vr^{\varepsilon} \tag{19}$$

$$\psi = (2\tilde{s})^{1/2}f(\eta) \tag{20}$$

$$u = u_e f'(\eta) \tag{21}$$

$$\beta = (1-\phi) = \beta_o B(\eta) \tag{22}$$

and

$$T = T_r\theta \tag{23}$$

In the above relations, $\tilde{s}$ and η are the transformed coordinates; while f, θ, and B are transformed dependent variables.

Application of the above similarity transforms to the governing equations resulted in the following:

a) Momentum Equation

$$B(\mu^* Bf'')' + Bff'' + \left[\frac{\rho_e}{\beta_o\rho_L} - B(f')^2\right]\frac{2\tilde{s}\,du_e}{u_e\,d\tilde{s}} = 0 \tag{24}$$

b) Energy Equation

$$(BK^*\theta')' + Pr_L f\theta' = 0 \tag{25}$$

c) Void Propagation Equation

$$B' + B\left(\frac{1}{\beta_o} - B\right)\frac{\theta'}{\theta} = 0 \tag{26}$$

where $\mu^* = \mu_m/\mu_r$, $K^* = K_e/K_L$, and Pr_L is the Prandtl Number of the liquid phase at the reference temperature, T_r.

In a similar manner, the boundary conditions were expressed in terms of the transformed variables. First the relations between the physical variables and the transformed variables were determined[4] as

$$f = \frac{-2[2\rho_L\mu_r\beta_o\int_0^x u_e r^{2\varepsilon}dx]^{1/2}}{\mu_r u_e r^{\varepsilon}\beta_o}\beta v \tag{27}$$

$$f' = u/u_e, \tag{28}$$

$$f'' = -\frac{[2\rho_L\mu_r\int_0^x u_e r^{2\varepsilon}dx]^{1/2}}{\mu_m\rho_L r^{\varepsilon}\beta}\tau \tag{29}$$

$$\theta = T/T_r, \tag{30}$$

$$\theta' = -\frac{[2\rho_L\mu_r\beta_o\int_0^x u_e r^{2\varepsilon}dx]^{1/2}}{K_e T_r\rho_L u_e r^{\varepsilon}\beta}q_c \tag{31}$$

and

$$B = \beta/\beta_o \tag{32}$$

Then the boundary conditions were transformed to give

at $\eta = 0$, $\theta = T_i/T_r$

$$f = -\frac{2[2\rho_L\mu_r\beta_o\int_0^x u_e r^{2\varepsilon}dx]^{1/2}}{\mu_r u_e r^{\varepsilon}\beta_o}\beta_i v_i \tag{33}$$

$$f'' = -\frac{[2\rho_L\mu_r\beta_o\int_0^x u_e r^{2\varepsilon}dx]^{1/2}}{\mu_m\rho_L r^{\varepsilon}\beta_i}\tau_i \tag{34}$$

and at $\eta \to -\infty$, $B = 1$; $f' = 0$; $\theta = T_o/T_r$

One of the most powerful techniques for solving Eq. (24)–26 is the recent quasilinearization method.[9] In applying this technique, an initial solution to the problem is first assumed and utilized to linearize the governing equations. The resulting equations represent a linear boundary-value problem which can be solved by classical numerical methods. An iteration approach is used to secure the converged and approximate answer to the problem. The details of the method as applied to the ablation problem described here are given by Hsieh.[4]

Stability and Convergence

Although the method of similarity transformation has been used extensively in studying the ablation process,[1-3] the stability and the convergence of the numerical solution of the transformed equations has not been shown previously. A serious error and inconsistent solution may result if the transformed variables and the boundary conditions are not chosen properly. In order to obtain a more accurate solution and a better algorithmic procedure, the stability and convergence of the transformed equations were considered in this study. The details are given by Hsieh.[4] The results may be summarized as follows: 1) it was found that the use of $T(-\infty) = T_o$ as a boundary condition for the energy equation permitted a satisfactory solution while the use of $\theta'(-\infty) = 0$ did not; 2) the use of θ defined as T/T_r rather than as $(T - T_o)/(T_r - T_o)$ avoided instability problems with the finite-difference form of the momentum equation; and 3) it was necessary to restrict solutions to a relatively small value for the product $(\rho_e/\rho_L)\theta(0)$ to insure stability.

Matching and Interface Conditions

The complete solution of an ablation process cannot be obtained unless the interface conditions between the gas boundary layer and the molten layer are matched. The first step in matching interface conditions is to select the appropriate solution for the gas boundary layer. During the past decade, a great number of papers dealing with the gas

boundary flow at the stagnation point of a blunt body were published.[10,11] For this particular application, the correlation equations presented by Bethe and Adams[12] are most suitable. Accordingly, the interface energy and shear stress transport are approximated by

$$q_i = q_s\psi = 0.7\left[\rho_s\mu_s\left(\frac{du_e}{dx}\right)_s\right]^{1/2}(h_s - h_i)Pr^{-2/3}\psi \qquad (35)$$

and

$$\tau_i = \tau_s\psi = \frac{q_s}{(h_s - h_i)}\left(\frac{du_e}{dx}\right)xPr^{2/3}\psi \qquad (36)$$

where

$$\psi = 1.0 - 0.68\,M^{0.26}(h_s - h_i)\dot{m}_i/q_s$$

The interface mass-transfer rate is the result of pyrolysis of resin, vaporization of silica, and the post-pyrolytic chemical reactions between carbon and silica. If the weight fraction of the ablative material converted into pyrolysis gases is w, the propagation of the void fraction is one-dimensional, and pyrolysis is at equilibrium, then the mass-transfer rate due to the pyrolysis can be related to the ablation rate, $\dot{m}_a$, as

$$\dot{m}_p = \frac{w}{1-w}\dot{m}_a = \frac{w}{1-w}\rho_L v_w(1-\phi) \qquad (37)$$

With an excess of silica, the overall post-pyrolytic reaction between carbon and silica can be represented as [4,13-17]

$$SiO_2 + C \rightarrow SiO_{(g)} + CO \qquad (38)$$

In utilizing this equation, it was assumed that the overall reaction could be considered as occurring near or at the surface of the molten layer. Also, the reactions were assumed to be controlled kinetically. The reaction rate was expressed as

$$\dot{m}_R = K_R\,e^{-E/RT} \qquad (39)$$

Neglecting the rate of silica vaporization, the total interface mass transfer is then

$$\dot{m}_i = \frac{w\rho_L v_w\beta}{1-w} + K_R\,e^{-E/RT} \qquad (40)$$

and the interface velocity of the liquid-phase is

$$v_i = \frac{\dot{m}_R}{\rho_L(1-\phi)} = \frac{K_R}{\rho_L(1-\phi)}\,e^{-E/RT} \qquad (41)$$

Another relation which is required for matching the interface conditions is the overall energy balance across the molten layer. In this analysis, it was plausible to consider that all the energy transferred to the surface of the molten layer was absorbed by the ablative material as sensible heat of the gas or liquid, the heat of the pyrolysis of the plastic, the heat of melting, and the heat of the carbon-silica reactions. The mathematical expression of this mechanism is

$$q_i = \dot{m}_p(Cp_G\,\Delta T + H_p) + \dot{m}_a(Cp_L\,\Delta T + H_f) + \dot{m}_R H_R \qquad (42)$$

where $\Delta T = T_i - T_o$ and it is assumed that all the ablating material reaches the interface temperature.

Because the solution of the numerical procedure can not be presented in explicit form, matching of the interface conditions was achieved by an iterative procedure. With assumed values for T_i and ψ, all the boundary conditions could be evaluated. Therefore, these two variables were chosen as parameters for the iteration. Since most of the physical values depended very strongly on T_i, it was used as the outside loop of the iteration. The value of ψ had a relatively insignificant influence on the solution and a converged value of ψ could be obtained in two to three iterations. The details of the iterative procedure are given by Hsieh.[4]

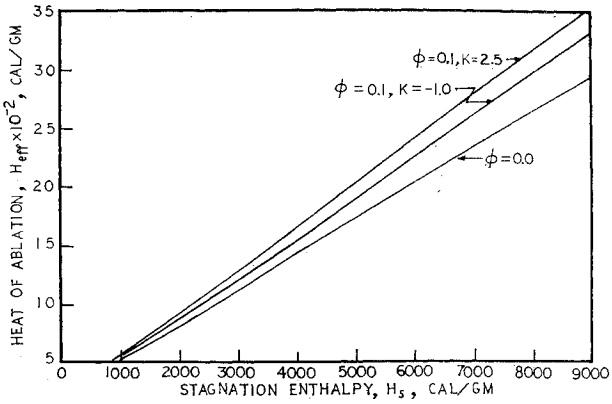

Fig. 3 Heat of ablation at different stagnation enthalpies and void fractions.

After a converged solution was obtained, the heat of ablation was determined by the following relation

$$H_{eff} = q_s(\dot{m}_a + \dot{m}_p) \qquad (43)$$

Results and Discussion

Numerical calculations based upon the procedure of this analysis were performed using a Univac 1108 digital computer for the surface ablation at the stagnation point of a blunt body. The distribution of the void fraction was assumed to be homogeneous.[4] The quasilinearization procedure was used to solve the resulting equations.[4] The numerical values of the physical properties and the environmental conditions used for the calculations were identical to those used by Hsieh and Seader[17] except that a value of 1.8×10^{-4} gm/cm^3 was used for the stagnation gas density. For each solution, ten different values of the interface temperature were chosen to cover an interval from 1650°K to 1950°K. The number of iterations extended from 3 at low interface temperatures up to 63 at higher interface temperatures. The computation time for all solutions was about 18 min.

The general properties of the solutions can be best characterized by Figs. 3–5. In Fig. 3, one can see that the heat of ablation increases as the stagnation enthalpy increases. This is due to the increase of the sensible heat of the molten layer, of the endothermic post-pyrolitic reactions, and the blocking effect caused by interface mass transfer. The heat of ablation increases when gas bubbles are present within the molten layer. This is especially true if the coefficient of the apparent viscosity is at the upper limit. Also the effect of the void fraction becomes more significant as the stagnation enthalpy increases.

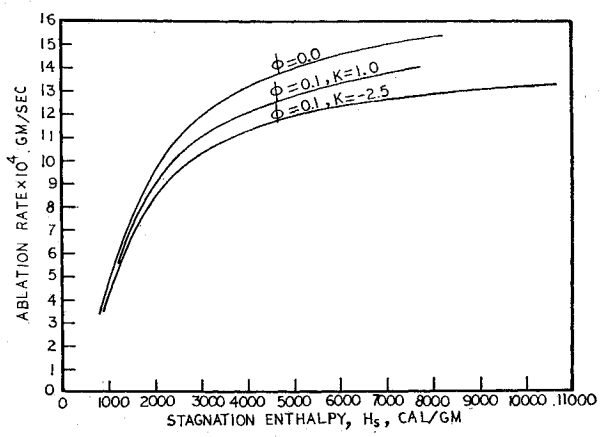

Fig. 4 Ablation rate at different stagnation enthalpies and void fractions.

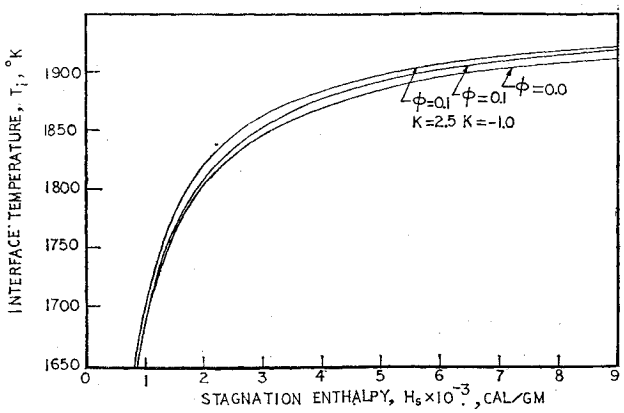

Fig. 5 Interface temperature at different stagnation enthalpies and void fractions.

The ablation rate increases with increasing stagnation enthalpy as shown in Fig. 4. Because of the rapid endothermic reactions and the highly effective blocking action at higher interface temperatures, the increase in ablation rate is relatively slower at the higher stagnation enthalpies. The effectiveness of the ablative material increases as the void fraction is increased to 0.1.

As expected, the interface temperature increases when the stagnation enthalpy increases, as shown in Fig. 5. Due to the exponential dependence of the reaction rate on the interface temperature, it eventually reaches a nearly constant value at large values of the stagnation enthalpy.

The general characteristics of the similarity-transform solution represented by Figs. 3–5 are in good agreement with the results obtained by the integration method.[17] Besides illustrating the solution of a specific ablation process, the numerical calculation presented here can also be applied to isolate and analyze the effect of each individual physical property on the overall performance of the ablative material. A detailed procedure for the perturbation method used is available.[4] Only some results are presented and discussed here.

From Figs. 6–8, it is seen that the distributions of $f(\eta)$, $f'(\eta)$, and $f''(\eta)$ reach their asymptotic values within a short dimensionless depth, η. This interval in the η-axis represents the thickness of the molten layer. In this study the profile of the temperature and the temperature gradient do not reach the asymptotic values within the range of the calculation. That is, the thickness of the thermal layer is much larger than that of the molten layer.

The rapid changes of the profiles of the axial velocity and its gradient at the high temperatures can be seen in Fig. 7 and 8. This tendency accounts for the unstable numerical calculation

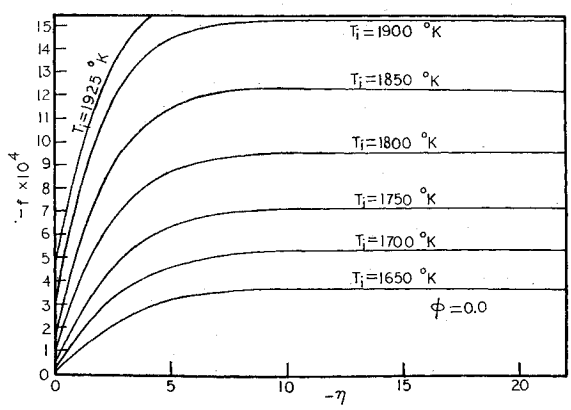

Fig. 6 Profile of the dimensionless stream function at various interface temperatures.

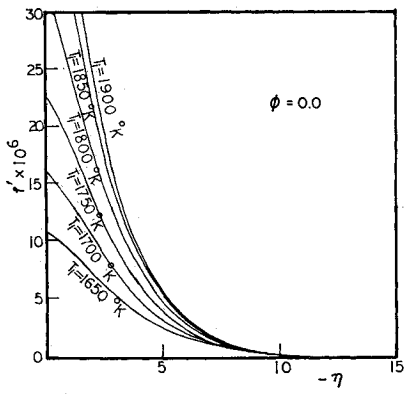

Fig. 7 Profile of the dimensionless velocity at various interface temperatures.

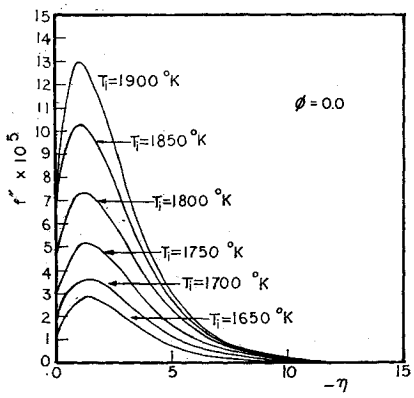

Fig. 8 Profile of the dimensionless velocity gradient.

at high temperatures. Note should be taken of the fact that neither the shear stress nor the momentum flux are proportional to the variation of $f''(\eta)$. However, the shear stress at any position can be calculated from Eq. (28) after replacing τ_i with τ.

Figs. 9 and 10 illustrate the dimensionless temperature profile and its gradient. Note that the value of $\theta'(\eta)$ is proportional to the conductive heat transfer rate. Thus, $\theta'(0)$ represents the conductive energy transfer at the interface. One interesting consequence of this fact is that the amount of energy transferred through the molten layer can be determined from Fig. 10. For example, for an interface temperature within the range of 1800°K to 1900°K, the value of $\theta'(\eta)$ at the point where $f'(\eta)$ approaches zero is only about seventy to eighty % of its value at the interface. Also, it is seen that the value of $\theta'(\eta)$ can only approach zero if the value of η is of the order of -100. The computation time to achieve this purpose would be extremely large and extravagant. The advantage of the algorithm developed in this analysis is, therefore, verified.

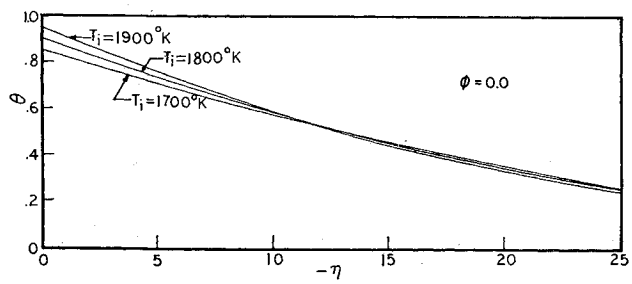

Fig. 9 Profile of the dimensionless temperature.

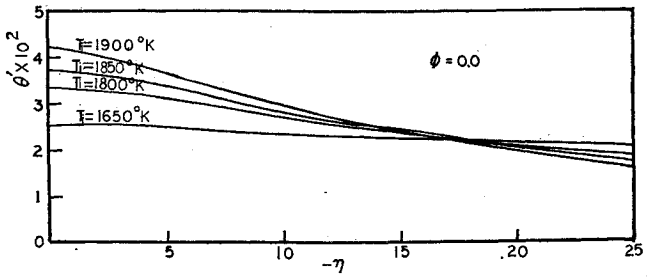

Fig. 10 Profile of the dimensionless temperature gradient.

Conclusion

Similarity transforms were used for solving the ablation process of silica-reinforced composites. With proper selection of the boundary conditions and the transformed variables, the technique of quasilinearization was utilized to obtain the solution of the transformed equations. The strategy of matching the interface conditions was also developed. By following the procedure, one can obtain the complete solution of an ablation process routinely. By analyzing the stability and convergence character of the numerical procedure, it was shown that this technique not only converges rapidly, but also yields a consistent and accurate solution.

References

[1] Sutton, G. W., "A Comparison of Several Approximate Theories of Melting Ablation," *Journal of Aeronautical Science*, Vol. 26, No. 6, June 1959, pp. 397–398.

[2] Sutton, G. W., "The Hydrodynamics and Heat Conduction of a Melting Surface," *Journal of Aeronautical Science*, Vol. 25, No. 1, Jan. 1958, pp. 29–32, 36.

[3] Chen, S. Y. and Allen, S. J., "Similarity Analysis for Transient Melting and Vaporization Ablation," *ARS Journal*, Vol. 32, No. 10, Oct. 1962, pp. 1536–1543.

[4] Hsieh, C., "Surface Ablation of Silica-Reinforced Composites," Ph. D. thesis, June 1973, Dept. of Chemical Engineering, Univ. of Utah, Salt Lake City, Utah.

[5] Zuber, N. and Staub, F. W., "The Propagation and the Wave Form of the Vapor Volumetric Concentration in Boiling Forced Convection System under Oscillatory Conditions," *International Journal of Heat and Mass Transfer*, Vol. 9, No. 9, Sept. 1966, pp. 871–895.

[6] Hinze, J. O., *Turbulence*, McGraw-Hill, New York, 1959, Chap. 5.

[7] Bankoff, C. G., "A Variable Density Single-Fluid Model for Two-Phase Flow with Particular Reference to Steam-Water Flow," *Transactions of the ASME, Journal of Heat Transfer*, Vol. 82, No. 4, Nov. 1960, pp. 265–272.

[8] Hansen, A. G., *Similarity Analysis of Boundary Value Problems in Engineering*, Prentice-Hall, New Jersey, 1964.

[9] Bellman, R. E. and Kalaba, R. E., *Quasilinearization and Nonlinear Boundary-Value Problems*, American Elsevier Publishing Co., New York, 1965.

[10] Baron, J. R., "The Binary Mixture Boundary Layer Associated with Mass Transfer Cooling at High Speeds," Rept. TR 160, May 1956, MIT Naval Supersonic Lab., Cambridge, Mass.

[11] Lees, L., "Convective Heat Transfer with Mass Addition and Chemical Reactions," *Third Combustion and Propulsion AGARD Colloquium*, Pergamon Press, New York, March 1958, pp. 451–498.

[12] Bethe, H. A. and Adams, M. C., "A Theory for Ablation of Glassy Materials," *Journal of Aeronautical Science*, Vol. 26, No. 6, June 1959, pp. 321–328, 350.

[13] Baird, J. D. and Taylor, J., "Reaction Between Silica and Carbon and the Activity of Silica in Slag Solution," *Transactions of the Faraday Society*, Vol. 54, 1958, pp. 526–539.

[14] Klinger, N., Strauss, E. L. and Kormarek, K. L. "Reactions Between Silica and Graphite," *Journal of the American Ceramic Society*, Vol. 49, No. 7, July 1966, pp. 369–375.

[15] Beecher, N. and Rosensweig, R. E., "Ablation Mechanisms in Plastics with Inorganic Reinforcement," *ARS Journal*, Vol. 31, No. 4, April 1961, pp. 532–539.

[16] Blumenthal, J. L., Santy, M. J. and Burns, E. A., "Kinetic Studies in Charred Silica-Reinforced Phenolic Resins," *AIAA Journal*, Vol. 4, No. 6, June 1966, pp. 1053–1057.

[17] Hsieh, C. and Seader, J. D., "Surface Ablation of Silica-Reinforced Composites," *AIAA Journal*, Vol. 11, No. 8, Aug. 1973, pp. 1181–1187.